Journal of Biomechanics 42 (2009) 884–890

Contents lists available at ScienceDirect

Journal of Biomechanics

journal homepage: www.elsevier.com/locate/jbiomech
www.JBiomech.com

Realistic loading conditions for upper body bending

A. Rohlmann *, T. Zander, M. Rao, G. Bergmann

Julius Wolff Institut, Charité—Universitätsmedizin Berlin, Augustenburger Platz 1, PSF 24, 13353 Berlin, Germany

ARTICLE INFO

Article history:
Accepted 20 January 2009

Keywords:
Lumbar spine
Load application mode
Intradiscal pressure
Intersegmental rotation
Finite element analysis

ABSTRACT

Different modes of load applications are used to simulate flexion and extension of the upper body. It is not clear which loading modes deliver realistic results and allow the comparison of different studies.

In a numerical study, a validated finite element model of the lumbar spine, ranging from the vertebra L1 to the disc L5–S1 was employed. Each of six different loading modes was studied for simulating flexion and extension, including pure moments, an eccentric axial force, using a wedged fixture, and applying upper body weight plus follower load plus muscle forces. Intersegmental rotations, intradiscal pressures and facet joint contact forces were calculated. Where possible, results were compared to data measured *in vivo*.

The results of the loading modes studied show a large variance for some values. Outcome measures such as flexion angle and intradiscal pressure differed at a segment by up to 44% and 88%, respectively, related to their maximum values. Intradiscal pressure is mainly determined by the magnitude of the applied compressive force. For flexion maximum contact forces between 0 and 69 N are predicted in each facet joint for different loading modes. For both flexion and extension, applying upper body weight plus follower load plus muscle forces as well as a follower load together with a bending moment delivers results which agreed well with *in vivo* data from the literature.

Choosing an adequate loading mode is important in spine biomechanics when realistic results are required for intersegmental rotations, intradiscal pressure and facet joint contact forces. Only then will results of different studies be comparable.

1. Introduction

The loading conditions within the spinal column are highly complex and have, therefore, not been fully characterized. Various simplifications have been made in experimental and numerical studies. It is not clear which modes of load application deliver realistic results.

Intersegmental angles in the lumbar spine have been determined from radiographs in neutral standing, flexion and extension of 89 subjects (Lin et al., 1994). Between standing and flexion they found the largest difference for segment L4–L5 and between standing and extension for segment L5–S1. Intradiscal pressure has been measured for several activities (Andersson et al., 1977; Nachemson, 1966; Sato et al., 1999; Schultz et al., 1982; Wilke et al., 1999).

Different loading modes were used for experimental and numerical studies. An axial force via an inclined loading plate has a shear component and can be used to generate flexion, extension or lateral bending (Adams et al., 1980; Pollintine et al., 2004). In this case, the moment along the specimen's length varies. An eccentric axial force causes a moment which results in bending of the spine (DiAngelo et al., 2002; Tai et al., 2008). When several segments are studied, the bending moment along the specimen or model may vary strongly, due to the spinal curvature and large deformations (Panjabi, 1988). Therefore, the application of pure moments was recommended when studying the spine. When it is applied at one end of a spinal specimen, it will be constantly transmitted through all levels. Mostly pure moments are applied to simulate flexion/extension, lateral bending and axial rotation. Very often a moment of 7.5 Nm is used for loading lumbar spine specimens or models (Niosi et al., 2006; Oxland et al., 1992; Panjabi et al., 1994; Rohlmann et al., 2001a; Wilke et al., 1998). Lower moments were chosen for osteoporotic specimens or when spinal defects were studied. In order to take the upper body weight into account, pure moments are often used in conjunction with a compressive force or a follower load (Niosi et al., 2006; O'leary et al., 2005; Ogon et al., 1997; Rahm and Hall, 1996; Rohlmann et al., 2006a; Schmidt et al., 2007; Wilke et al., 2001b; Zander et al., 2001).

A follower load stabilizes the spine and allows the application of high loads (Patwardhan et al., 1999; Rohlmann et al., 2001b). It follows the curvature of the spine through the proximities of the centres of rotations. The most cranial vertebra is loaded with a compressive force and the other vertebrae with a small correcting force facing to the centre of the local spinal curvature. Follower

* Corresponding author. Tel.: +49 30 450559083; fax: +49 30 450559980.
E-mail address: rohlmann@biomechanik.de (A. Rohlmann).

0021-9290/$ - see front matter © 2009 Elsevier Ltd. All rights reserved.
doi:10.1016/j.jbiomech.2009.01.017

loads have been used by several groups, often in combination with pure moments (Goel et al., 2005, 2006; Renner et al., 2007; Rohlmann et al., 2001b) or muscle forces (Rohlmann et al., 2006a, b, c; Wilke et al., 2003).

Muscle forces are difficult to apply in experimental studies. Thus, only few groups applied muscle forces in *in vitro* studies (Panjabi et al., 1989; Quint et al., 1998; Wilke et al., 2003). Mostly the effect of muscle forces is tried to be obtained by applying an axial force, e.g., a follower load, an axial preload or an off-centred compressive load. The magnitude of the load may vary considerably. In finite element studies, the application of a great number of muscle forces is not a problem, but still seldom used (Calisse et al., 1999; Zander et al., 2001) as the muscle forces are not known. The influence of muscle forces on the biomechanical behaviour of the lumbar spine was investigated using the finite element method (Goel et al., 1993; Shirazi-Adl and Parnianpour, 1996). Finite element models were also used to estimate muscle forces for motion in the sagittal plane (Calisse et al., 1999; Rohlmann et al., 2006a; Zander et al., 2001).

Panjabi (Goel et al., 2005; Panjabi, 2007) introduced a hybrid approach for testing adjacent segments after insertion of spinal implants: First, the intact spine is tested with a pure moment and the total rotation angle is determined. After insertion of the implant, the specimen or model is loaded with an increasing pure moment until the total rotation angle of the intact spine is reached. This way the overall deformation before and after implantation is the same. The principle of the hybrid method can also be used when a follower load in combination with a moment is used instead of an implant.

In the present study, different loading modes, simulating flexion and extension of the upper body without an additionally carried external weight, were studied using a finite element model of the intact lumbar spine to calculate intersegmental rotation (ISR), intradiscal pressure (IDP) and facet joint contact forces (FJCF). These results were compared with those of *in vivo* studies to show how the results differ for the various loading modes. We also showed which loading modes deliver most realistic biomechanical results and should thus be preferred.

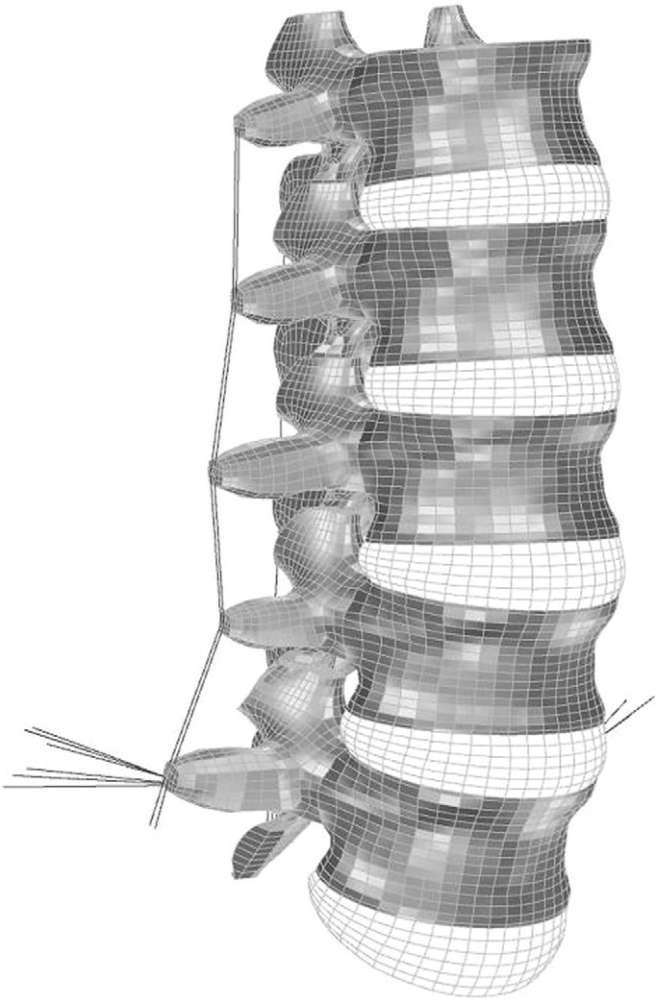

Fig. 1. Finite element model of the lumbar spine.

2. Methods

2.1. Finite element model of intact lumbar spine

A non-linear finite element model of the lumbar spine was used. It consisted of 5 vertebrae, the connecting intervertebral discs and all ligaments of the lumbar spine (Fig. 1). The facet joints were curved, had a gap of 0.5 mm before loading was applied and a thin cartilaginous layer. Thus, facet joint contact force was zero as long as there was a gap. The cartilaginous layer had a total thickness of 0.5 mm and was simulated using soft contact with an exponentially increasing contact force during decreasing contact distance (Sharma et al., 1995). After a compression of the cartilaginous layer of 0.5 mm, the joint reached the same stiffness as the surrounding bone. The facet joints could transmit only compressive forces. The annulus fibrosis of the discs was modelled as fibre-reinforced hyperelastic composite (Eberlein et al., 2000). The fibres were embedded in the ground substance in concentric rings around the nucleus. The nuclei pulposi were modelled as incompressible fluid-filled cavities. The ligaments were represented by tension—only spring elements with non-linear material properties. The material properties of the different tissues were taken from the literature and are given in a similar paper where the loading case standing is studied (Rohlmann et al., submitted). The inferior side of the lumbosacral disc was rigidly fixed. The model was calibrated using experimental data for different anatomical-reduction levels, loading directions and magnitudes (Heuer et al., 2007) and validated extensively (Rohlmann et al., 2006a; Zander et al., 2007, 2001) for ISR and IDP using the experimental data (Heuer et al., 2007; Rohlmann et al., 2001a, b; Wilke et al., 1999). The finite element model has been described in detail elsewhere (Rohlmann et al., 2005; Zander et al., 2001).

2.2. Simulated loads

The activities of flexion and extension of the upper body without an additional external load like carrying a weight were studied.

2.2.1. Flexion (extension)

Flexion of the upper body was simulated by applying to the L1 vertebra (Fig. 2)

(A) a pure moment of 7.5 Nm. L1 was unconstrained i.e. translation and rotation was allowed;
(B) an eccentric force of 75 N at a lever arm of 100 mm, causing a moment of 7.5 Nm at L1. L1 was unconstrained;
(C) a pure moment of 7.5 Nm after a follower load of 500 N was applied. L1 was unconstrained.

In addition, flexion (extension) was simulated by

(D) a hybrid approach for the loading mode pure moment plus follower load similar to the hybrid approach described by Panjabi (2007). First a follower load of 500 N was applied. Then an additional pure moment was applied until the total segmental rotation was the same as for the mode (A). The required moment in this case was 7.65 Nm (4.99 Nm). L1 was unconstrained;
(E) an axial force of 500 N applied via a rigid-wedged fixture causing a flexion (extension) angle of 30° (20°) of the L1 vertebra;
(F) an upper body weight of 260 N acting at the centre of gravity 30 mm anteriorly and 200 mm cranially of the T12–L1 disc centre, plus a follower load of 200 N plus a force in the erector spinae (rectus abdominis), chosen as to cause a flexion (extension) angle of 30° (20°) (Rohlmann et al., 2006a).

2.3. Evaluation

ISRs, IDPs and FJCF were calculated. Intersegmental angles in the lumbar spine have been determined from radiographs in neutral standing, flexion and extension (Lin et al., 1994). The differences between the mean values for standing, flexion and extension were calculated for each segment to determine the ISRs due to flexion and due to extension. The total flexion (extension) angle differed between the experimental and numerical studies. Therefore, the ratio of the total flexion

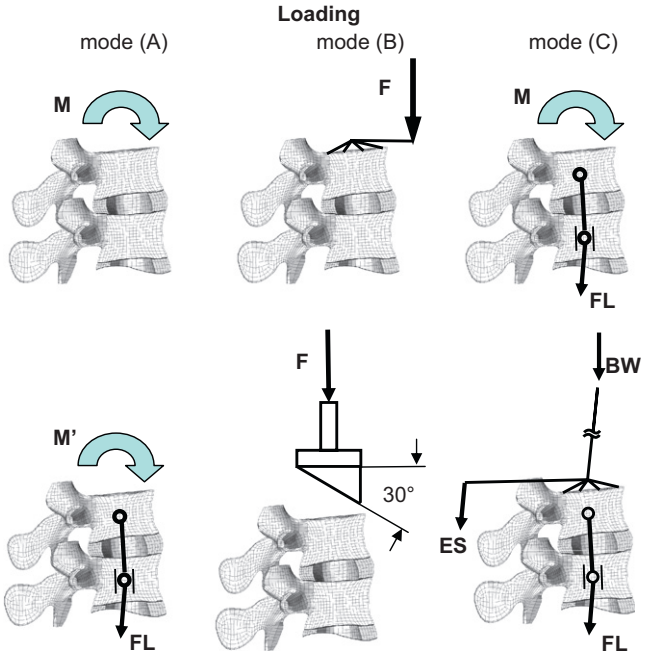

Fig. 2. Schematic sketch of the loading modes simulating flexion. M and M' = bending moments, F = axial force, FL = follower load; BW = upper body weight; ES = force in m. erector spinae.

(extension) angles taken from the experimental and numerical method was determined for each loading mode. This ratio was used to adjust the experimentally determined relative rotation angles at each level in order to achieve the same amount of total flexion (extension) for both methods. With these data, the sum of the absolute differences between calculated and measured ISR as well as the average deviation from the mean difference between calculated and measured ISR were determined. These values are measures for the shape of the lumbar spine. The calculated IDPs were compared to values measured *in vivo* and the differences are determined. At level L4–L5, the mean pressure value of the two *in vivo* studies (Sato et al., 1999; Wilke et al., 1999) was chosen as a reference value. FJCF normal to the facet surfaces were calculated. The average force of the left and right facet joint is presented.

The finite element program ABAQUS, version 6.6-3 (Dassault Systèmes, Versailles, France), was used together with the pre- and post-processor MSC/PATRAN (MSC Software, Marburg, Germany).

3. Results

3.1. Flexion of the upper body

ISR is mostly between 5° and 6° at each level for the loading modes (A)–(D) (Fig. 3). For the loading modes axial force via a 30°-wedged fixture (mode (E)) and when muscle forces are applied (mode (F)), ISR increases from cranial to caudal. The smallest rotation is 1.7° at level L1–L2 for loading mode (E) and the highest rotation is 8.9° at level L5–S1 for the same loading mode. There are only minor differences in ISR between the pure moment with follower load (mode (C)) and the hybrid moment with follower load (mode (D)). The sum of the absolute differences between calculated and measured ISR varies between 6.0° (mode (F)) and 9.5° (mode (A)), while the average deviation from the mean difference is 2.0° or less for all loading modes (Table 1).

IDP varies strongly for the different loading modes (Fig. 4). The pressure is lesser than 0.3 MPa for the loading modes (A) and (B). When a follower load is applied (modes (C) and (D), IDP at the various levels varies between 0.52 and 0.59 MPa. IDP increases from cranial to caudal, when an axial force via a wedged fixture is applied (mode (E)). The highest pressure is predicted for applying the upper body weight plus a follower load plus a muscle force (mode (F)). The maximum value is 1.51 MPa at level L5–S1, and 1.28 MPa at L4–L5. For comparison, IDP measured *in vivo* was 1.04 MPa at level L3–L4, and between 1.1 and 1.32 MPa at level L4–L5. The pressure measured in volunteers is more than 8 times higher than that found for the loading modes where pure moments were applied (mode (A)). Differences between the calculated and the *in vivo*-measured IDPs are less than 0.2 MPa only for the loading mode (F) and about 1 MPa for the modes (A) and (B) (Table 1).

FJCF was found to be zero at all levels for the loading modes (A) to (D). An axial force via a 30°-wedged fixture (mode (E)) leads to increasing contact forces from cranial to caudal. The predicted force is 13 N at level L1–L2 and 69 N at level L5–S1. When muscle forces were applied (mode (F)), a non-zero FJCF is predicted only at the level L5–S1 (24 N).

3.2. Extension of the upper body

ISR varies between 2.8° and 5.1° for the different loading modes and levels (Fig. 5). The highest value is predicted at level L1–L2 when a pure moment with follower load (mode (C)) is applied. The smallest differences for the 6 loading modes are calculated at level L5–S1. The calculated values differ up to 4.2° from the mean values measured *in vivo* (Table 2). The average deviation from the mean difference between calculated and measured ISR is between 1.9° and 2.5° for the different loading modes which is less than 1 standard deviation for the measured values. The sum of the absolute differences between calculated and measured ISR varies between 7.1° and 9.1° (Table 2).

IDP is low (between 0.20 and 0.34 MPa) for the loading modes (A) and (B) and between 0.44 and 0.65 MPa for the other four loading modes (Fig. 6). The values measured *in vivo* at level L4–L5 were 0.59 and 0.60 (Sato et al., 1999; Wilke et al., 2001a). Thus, the differences between numerical and measured values are 0.05 or less for the loading modes (C)–(F) and 0.29 MPa or more for the loading modes (A) and (B) (Table 2).

FJCF are highest at levels L2–L3 to L5–S1 for loading mode (E) (Fig. 7 and Table 2). The maximum value is 117 N. The lowest forces are predicted for the modes (A) and (D).

4. Discussion

The effects of different loading modes simulating flexion and extension of the upper body on ISR, IDP and FJCF were determined.

This study has some limitations as all finite element studies in spine biomechanics. The flexion and extension angles differed in the experimental studies from those in the present one. For the ISR a linear extrapolation was performed. Also the shapes of the lumbar spines of the volunteers in the *in vivo* studies are not known and may differ from that in the present numerical study. In the loading modes (A)–(D), the deformation depended on the applied load. In the other two loading modes the overall deformation of the model was predetermined. That value is slightly greater than the overall deformation when the load was predetermined. However, both the applied moment of 7.5 Nm and the predetermined flexion angle of 30° are frequently used in experimental and numerical studies. The literature values for *in vivo* measured IDP have been found for only one (extension) or two levels (flexion). These measurements have been performed in 1–8 volunteers which may indeed not be representative for an average person. Several assumptions and simplifications were necessary for creating the finite element model. Therefore, the absolute values calculated may not be representative for an

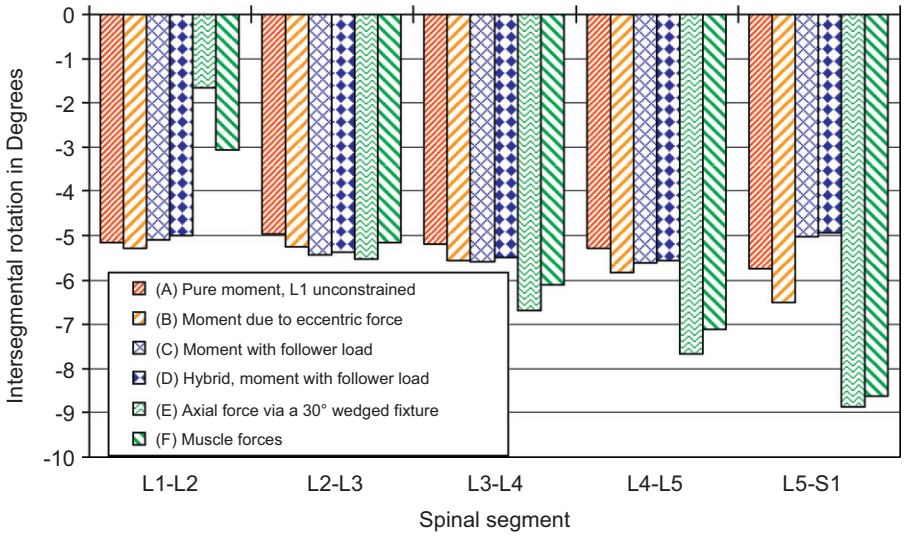

Fig. 3. Intersegmental rotations for different loading modes simulating flexion of the upper body.

Table 1
Comparison of several parameters for the six loading modes simulating upper body flexion.

Parameter	Loading					
	Mode (a)	Mode (B)	Mode (C)	Mode (D)	Mode (E)	Mode (F)
Difference between numerical and *in vivo* values for ISR at L1–L2 in degrees	−0.9	−1.3	−0.8	−0.7	2.2	0.7
Difference between numerical and *in vivo* values for ISR at L2–L3 in degrees	0.8	0.2	0.4	0.4	−0.4	−0.1
Difference between numerical and *in vivo* values for ISR at L3–L4 in degrees	2.8	1.9	2.4	2.5	0.3	0.9
Difference between numerical and *in vivo* values for ISR at L4–L5 in degrees	4.3	3.1	4.0	4.1	0.7	1.3
Difference between numerical and *in vivo* values for ISR at L5–S1 in degrees	0.7	−0.6	1.4	1.5	−3.3	−3.0
Sum of absolute differences between calculated and measured ISR in degrees	9.5	**7.0**	8.9	9.2	**6.9**	**6.0**
Average deviation from mean difference between calculated and measured ISR in degrees	**2.0**	**1.8**	**1.8**	**1.8**	**2.0**	**1.7**
Difference of IDP between numerical and *in vivo* values for L3–L4 in MPa	0.91	0.83	0.51	0.52	0.38	**−0.18**
Difference of IDP between numerical and *in vivo* values for L4–L5 in MPa	1.08	0.97	0.69	0.69	0.41	**−0.07**
Maximum facet joint force in N	**0**	**0**	**0**	**0**	69	24

ISR = intersegmental rotation; IDP = intradiscal pressure; bold values represent good agreement with *in vivo* results.

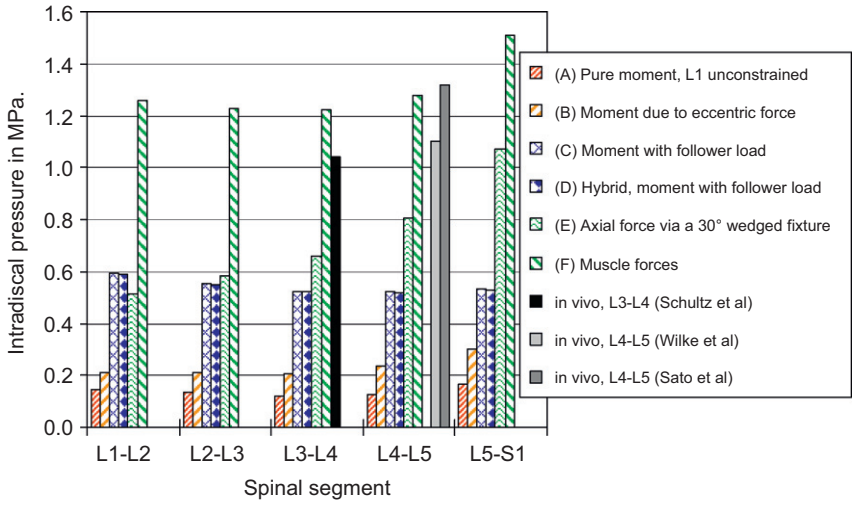

Fig. 4. Comparison of calculated and measured intradiscal pressures for different loading modes simulating flexion of the upper body.

average person. However, the principal effect of the different loading modes remains unaffected, since the same model was used for all the loading modes.

No additional external loads, e.g., carrying a weight, were considered in the present study. They would lead to higher muscle activation resulting in an increased axial spinal compressive force.

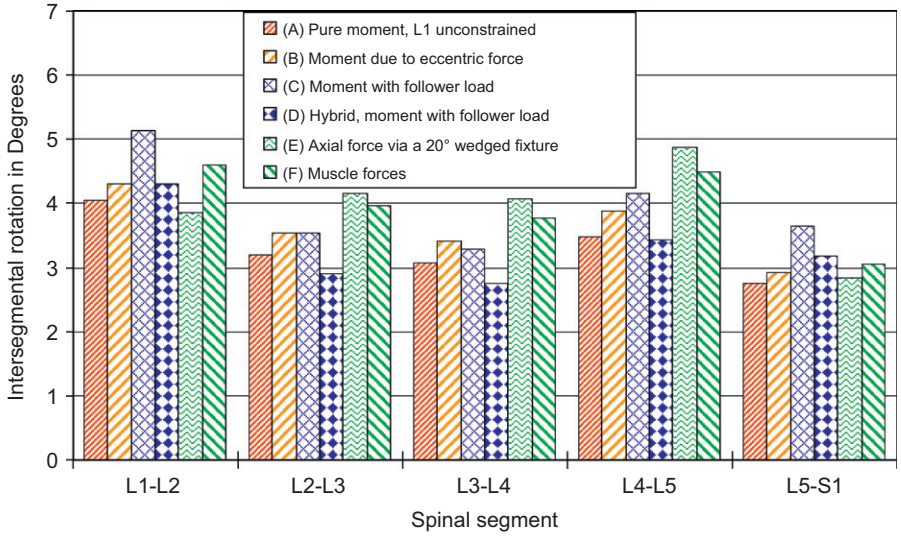

Fig. 5. Intersegmental rotations for different loading modes simulating extension of the upper body.

Table 2
Comparison of several parameters for the six loading modes simulating upper body extension.

Parameter	Loading					
	Mode (A)	Mode (B)	Mode (C)	Mode (D)	Mode (E)	Mode (F)
Difference between numerical and *in vivo* values for ISR at L1–L2 in degrees	2.0	2.1	2.7	2.2	1.4	2.1
Difference between numerical and *in vivo* values for ISR at L2–L3 in degrees	1.3	1.5	1.3	1.0	1.9	1.7
Difference between numerical and *in vivo* values for ISR at L3–L4 in degrees	−0.5	−0.5	−1.0	−0.9	−0.3	−0.6
Difference between numerical and *in vivo* values for ISR at L4–L5 in degrees	0.4	0.5	0.5	0.3	1.2	0.8
Difference between numerical and *in vivo* values for ISR at L5–S1 in degrees	−3.1	−3.5	−3.4	−2.7	−4.2	−4.0
Sum of absolute differences between calculated and measured ISR in degrees	**7.3**	8.0	8.8	**7.1**	8.9	9.1
Average deviation from mean difference between calculated and measured ISR in degrees	**2.0**	**2.2**	**2.3**	**1.9**	**2.5**	**2.5**
Difference of IDP between numerical and *in vivo* values for L4–L5 in MPa	0.37	0.29	**0.01**	**0.05**	**−0.03**	**−0.01**
Maximum facet joint force in N	43	58	86	50	117	94

ISR = intersegmental rotation; IDP = intradiscal pressure; bold values represent good agreement with *in vivo* results.

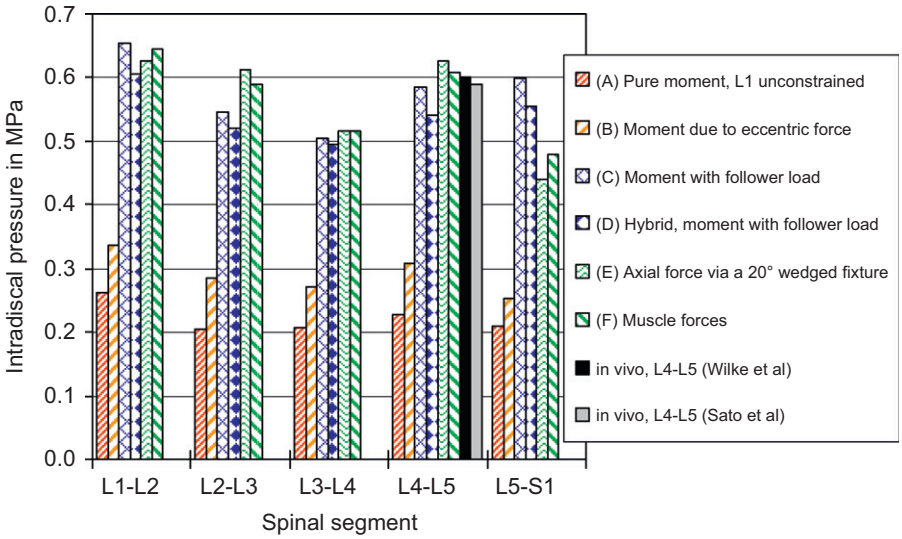

Fig. 6. Comparison of calculated and measured intradiscal pressure for different loading modes simulating extension of the upper body.

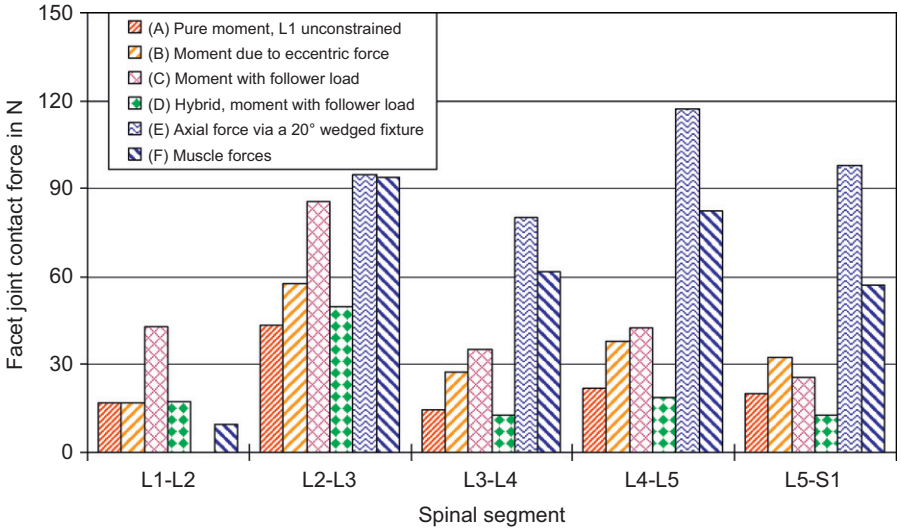

Fig. 7. Contact forces in the facet joints for different loading modes simulating extension.

External forces may have different magnitudes and lever arms. The investigation of these effects necessitates additional studies.

Flexion and extension cause characteristic distributions of ISR in the lumbar spine (Lin et al., 1994). For the studied loading modes the sum of the absolute differences between calculated and measured ISR during flexion varied between 6.0° for mode (F) and 9.5° for mode (A) (Table 1). During extension it varied between 7.1° for mode (D) and 9.1° for mode (F) (Table 2). The average deviations from the mean differences between numerical and experimental ISR were similar for all loading modes simulating flexion and extension and less than 1 standard deviation of the measured values. At single segments, the differences were always less than 1 standard deviation for all loading modes except for flexion for one segment each for the modes (A), (C) and (D).

IDP is very low when only pure moments (mode (A)) are applied (Figs. 4 and 6). Low values are also predicted when the moment was caused by an eccentric force (mode (B)), since the eccentric force was only 75 N at a lever arm of 100 mm. For flexion, values similar to those measured in volunteers are predicted only when muscle forces were applied (Fig. 3 and Table 1). A follower load of 500 N, which delivers realistic pressure values for standing, is not sufficient for simulating flexion with respect to IDP, since it does not take into account the global muscle force required for stabilizing the flexed upper body. However, when the follower load was increased to 1175 N (which we tested additionally) in the loading modes (C) and (D) the IDP at levels L3–L4 and L4–L5 increased to 1.1 MPa which is the median value of the measured IDP (Sato et al., 1999; Wilke et al., 1999). This increase had only a minor effect on ISR and no effect on calculated FJCF. For extension, the IDP varied only slightly for the modes (C)–(F) and they were similar to the ones measured *in vivo* (Sato et al., 1999; Wilke et al., 2001a) (Fig. 6, Table 3).

During flexion of the upper body, the gap size of the facet joints is normally increased. Thus, the contact force should be small or zero for this loading mode. However, when flexion is simulated by using a 30° wedge fixture, contact forces up to 69 N are predicted. Thus, this loading mode seems to be rather unsuited in studies where the FJCF are pertinent. In contrast, the facet joints are loaded during extension. The maximum FJCF varied between 43 N (mode (A)) and 117 N (mode (E)). No *in vivo* data for this force is available. In an *in vitro* study Wilson et al. (2006) applied an extension moment of 7.5 Nm and measured FJCF between 10 and 50 N. All calculated FJCF are within the physiological range although the values for loading mode (E) seem to be quite high.

In conclusion, for *flexion,* the smallest differences in ISR between numerical and *in vivo* values were found when muscle forces were assumed (mode (F)). However, the other loading modes also delivered reasonable results, although differences in ISR up to 4° within one segment were calculated. The loading mode (F) also showed the smallest differences in IDP, but a good agreement with *in vivo* results is also achieved when the follower load is increased to 1175 N in modes (C) and (D), when flexion is simulated. Regarding FJCF, expected results are predicted for modes (A)–(D). In summary, when only motion is important, in our opinion all studied loading modes simulating flexion deliver acceptable results. When IDP is deemed important, the loading mode (F) and modified modes (C) and (D) deliver realistic values. For studying FJCF, loading mode (E) appears to be not realistic.

For *extension*, the smallest differences in ISR between calculated and measured values were found when the hybrid method with follower load (mode (D)) and a pure moment (mode (A)) were applied. However, the differences between the six loading modes are small. Regarding IDP, the modes (C)–(F) deliver realistic values while the IDP for the other two modes is much too low. The FJCF seems to be somewhat high when using a wedged fixture (mode (E)). Thus for the modes (C), (D) and (F) realistic results can be expected when simulating extension.

Very few *in vivo* data exists for *lateral bending* of the spine. For motion in the sagittal plane, good agreement with *in vivo* data could be achieved when a follower load superimposed by a pure bending moment was applied. Thus, it seems reasonable that this concept also delivers realistic results for lateral bending. The centre of gravity of the upper body weight is only slightly changed during lateral bending. Therefore, for *lateral bending* we suggest a follower load of 500 N and a superimposed bending moment for this loading case.

Conflict of interest

None of the authors have a conflict of interest regarding the subject matter of this manuscript.

Acknowledgement

This study has been supported by the Deutsche Forschungsgemeinschaft (Ro 581/17-2). Finite element calculations were performed at Norddeutscher Verbund für Hoch und Höchstleistungsrechnen (HLRN). The authors thank Nagananda K. Burra for the computational assistance.

References

Adams, M.A., Hutton, W.C., Stott, J.R., 1980. The resistance to flexion of the lumbar intervertebral joint. Spine 5, 245–253.

Andersson, G.B., Ortengren, R., Nachemson, A., 1977. Intradiskal pressure, intra-abdominal pressure and myoelectric back muscle activity related to posture and loading. Clinical Orthopaedics and Related Research 129, 156–164.

Calisse, J., Rohlmann, A., Bergmann, G., 1999. Estimation of trunk muscle forces using the finite element method and in vivo loads measured by telemeterized internal spinal fixation devices. Journal of Biomechanics 32, 727–731.

DiAngelo, D.J., Scifert, J.L., Kitchel, S., Cornwall, G.B., McVay, B.J., 2002. Bioabsorbable anterior lumbar plate fixation in conjunction with cage-assisted anterior interbody fusion. Journal of Neurosurgery 97, 447–455.

Eberlein, R., Holzapfel, G.A., Schulze-Bauer, C.A.J., 2000. An anisotropic model for annulus tissue and enhanced finite element analysis of intact lumbar disc bodies. Computer Methods in Biomechanics and Biomedical Engineering 4, 209–229.

Goel, V.K., Grauer, J.N., Patel, T., Biyani, A., Sairyo, K., Vishnubhotla, S., Matyas, A., Cowgill, I., Shaw, M., Long, R., Dick, D., Panjabi, M.M., Serhan, H., 2005. Effects of charite artificial disc on the implanted and adjacent spinal segments mechanics using a hybrid testing protocol. Spine 30, 2755–2764.

Goel, V.K., Kong, W., Han, J.S., Weinstein, J.N., Gilbertson, L.G., 1993. A combined finite element and optimization investigation of lumbar spine mechanics with and without muscles. Spine 18, 1531–1541.

Goel, V.K., Panjabi, M.M., Patwardhan, A.G., Dooris, A.P., Serhan, H., 2006. Test protocols for evaluation of spinal implants. Journal of Bone and Joint Surgery 88 (Suppl 2), 103–109.

Heuer, F., Schmidt, H., Klezl, Z., Claes, L., Wilke, H.J., 2007. Stepwise reduction of functional spinal structures increase range of motion and change lordosis angle. Journal of Biomechanics 40, 271–280.

Lin, R.M., Yu, C.Y., Chang, Z.J., Lee, C.C., Su, F.C., 1994. Flexion-extension rhythm in the lumbosacral spine. Spine 19, 2204–2209.

Nachemson, A., 1966. The load on lumbar disks in different positions of the body. Clinical Orthopaedics and Related Research 45, 107–122.

Niosi, C.A., Zhu, Q.A., Wilson, D.C., Keynan, O., Wilson, D.R., Oxland, T.R., 2006. Biomechanical characterization of the three-dimensional kinematic behaviour of the Dynesys dynamic stabilization system: an in vitro study. European Spine Journal 15, 913–922.

O'Leary, P., Nicolakis, M., Lorenz, M.A., Voronov, L.I., Zindrick, M.R., Ghanayem, A., Havey, R.M., Carandang, G., Sartori, M., Gaitanis, I.N., Fronczak, S., Patwardhan, A.G., 2005. Response of Charite total disc replacement under physiologic loads: prosthesis component motion patterns. Spine Journal 5, 590–599.

Ogon, M., Bender, B.R., Hooper, D.M., Spratt, K.F., Goel, V.K., Wilder, D.G., Pope, M.H., 1997. A dynamic approach to spinal instability. Part I: sensitization of intersegmental motion profiles to motion direction and load condition by instability. Spine 22, 2841–2858.

Oxland, T.R., Lin, R.M., Panjabi, M.M., 1992. Three-dimensional mechanical properties of the thoracolumbar junction. Journal of Orthopaedic Research 10, 573–580.

Panjabi, M., Abumi, K., Duranceau, J., Oxland, T., 1989. Spinal stability and intersegmental muscle forces. A biomechanical model. Spine 14, 194–200.

Panjabi, M.M., 1988. Biomechanical evaluation of spinal fixation devices: I. A conceptual framework. Spine 13, 1129–1134.

Panjabi, M.M., 2007. Hybrid multidirectional test method to evaluate spinal adjacent-level effects. Clinical Biomechanics 22, 257–265.

Panjabi, M.M., Oxland, T.R., Yamamoto, I., Crisco, J.J., 1994. Mechanical behavior of the human lumbar and lumbosacral spine as shown by three-dimensional load–displacement curves. Journal of Bone and Joint Surgery 76-A, 413–424.

Patwardhan, A.G., Havey, R.M., Meade, K.P., Lee, B., Dunlap, B., 1999. A follower load increases the load-carrying capacity of the lumbar spine in compression. Spine 24, 1003–1009.

Pollintine, P., Dolan, P., Tobias, J.H., Adams, M.A., 2004. Intervertebral disc degeneration can lead to "stress-shielding" of the anterior vertebral body: a cause of osteoporotic vertebral fracture? Spine 29, 774–782.

Quint, U., Wilke, H.J., Loer, F., Claes, L., 1998. Laminectomy and functional impairment of the lumbar spine: the importance of muscle forces in flexible and rigid instrumented stabilization—a biomechanical study in vitro. European Spine Journal 7, 229–238.

Rahm, M.D., Hall, B.B., 1996. Adjacent-segment degeneration after lumbar fusion with instrumentation: a retrospective study. Journal of Spinal Disorders 9, 392–400.

Renner, S.M., Natarajan, R.N., Patwardhan, A.G., Havey, R.M., Voronov, L.I., Guo, B.Y., Andersson, G.B., An, H.S., 2007. Novel model to analyze the effect of a large compressive follower pre-load on range of motions in a lumbar spine. Journal of Biomechanics 40, 1326–1332.

Rohlmann, A., Bauer, L., Zander, T., Bergmann, G., Wilke, H.J., 2006a. Determination of trunk muscle forces for flexion and extension by using a validated finite element model of the lumbar spine and measured in vivo data. Journal of Biomechanics 39, 981–989.

Rohlmann, A., Neller, S., Bergmann, G., Graichen, F., Claes, L., Wilke, H.-J., 2001a. Effect of an internal fixator and a bone graft on intersegmental spinal motion and intradiscal pressure in the adjacent regions. European Spine Journal 10, 301–308.

Rohlmann, A., Neller, S., Claes, L., Bergmann, G., Wilke, H.-J., 2001b. Influence of a follower load on intradiscal pressure and intersegmental rotation of the lumbar spine. Spine 26, E557–E561.

Rohlmann, A., Zander, T., Bergmann, G., 2005. Effect of total disc replacement with ProDisc on the biomechanical behavior of the lumbar spine. Spine 30, 738–743.

Rohlmann, A., Zander, T., Bergmann, G., 2006b. Effects of fusion-bone stiffness on the mechanical behavior of the lumbar spine after vertebral body replacement. Clinical Biomechanics 21, 221–227.

Rohlmann, A., Zander, T., Bergmann, G., 2006c. Spinal loads after osteoporotic vertebral fractures treated by vertebroplasty or kyphoplasty. European Spine Journal 15, 1255–1264.

Rohlmann, A., Zander, T., Rao, M., Bergmann, G., Applying a follower load delivers realistic results for simulating standing. Journal of Biomechanics, submitted for publication.

Sato, K., Kikuchi, S., Yonezawa, T., 1999. In vivo intradiscal pressure measurement in healthy individuals and in patients with ongoing back problems. Spine 24, 2468–2474.

Schmidt, H., Kettler, A., Heuer, F., Simon, U., Claes, L., Wilke, H.J., 2007. Intradiscal pressure, shear strain, and fiber strain in the intervertebral disc under combined loading. Spine 32, 748–755.

Schultz, A., Andersson, G., Ortengren, R., Haderspeck, K., Nachemson, A., 1982. Loads on the lumbar spine. Validation of a biomechanical analysis by measurements of intradiscal pressures and myoelectric signals. Journal of Bone and Joint Surgery 64-A, 713–720.

Sharma, M., Langrana, N.A., Rodriguez, J., 1995. Role of ligaments and facets in lumbar spinal stability. Spine 20, 887–900.

Shirazi-Adl, A., Parnianpour, M., 1996. Role of posture in mechanics of the lumbar spine in compression. Journal of Spinal Disorders 9, 277–286.

Tai, C.L., Hsieh, P.H., Chen, W.P., Chen, L.H., Chen, W.J., Lai, P.L., 2008. Biomechanical comparison of lumbar spine instability between laminectomy and bilateral laminotomy for spinal stenosis syndrome—an experimental study in porcine model. BMC Musculoskeletal Disorders 9, 84.

Wilke, H.-J., Neef, P., Caimi, M., Hoogland, T., Claes, L.E., 1999. New in vivo measurements of pressures in the intervertebral disc in daily life. Spine 24, 755–762.

Wilke, H.-J., Neef, P., Hinz, B., Seidel, H., Claes, L., 2001a. Intradiscal pressure together with anthropometric data—a data set for the validation of models. Clinical Biomechanics 16, S111–S126.

Wilke, H.J., Rohlmann, A., Neller, S., Graichen, F., Claes, L., Bergmann, G., 2003. ISSLS prize winner: a novel approach to determine trunk muscle forces during flexion and extension: a comparison of data from an in vitro experiment and in vivo measurements. Spine 28, 2585–2593.

Wilke, H.J., Rohlmann, A., Neller, S., Schultheiss, M., Bergmann, G., Graichen, F., Claes, L.E., 2001b. Is it possible to simulate physiologic loading conditions by applying pure moments? A comparison of in vivo and in vitro load components in an internal fixator. Spine 26, 636–642.

Wilke, H.J., Wenger, K., Claes, L., 1998. Testing criteria for spinal implants: recommendations for the standardization of in vitro stability testing of spinal implants. European Spine Journal 7, 148–154.

Wilson, D.C., Niosi, C.A., Zhu, Q.A., Oxland, T.R., Wilson, D.R., 2006. Accuracy and repeatability of a new method for measuring facet loads in the lumbar spine. Journal of Biomechanics 39, 348–353.

Zander, T., Rohlmann, A., Bock, B., Bergmann, G., 2007. Biomechanische Konsequenzen von verschiedenen Positionierungen bewegungserhaltender Bandscheibenimplantate. Eine Finite-Elemente-Studie an der Lendenwirbelsäule. Orthopade 36, 205–211.

Zander, T., Rohlmann, A., Calisse, J., Bergmann, G., 2001. Estimation of muscle forces in the lumbar spine during upper-body inclination. Clinical Biomechanics 16, S73–S80.